

HST AND *Spitzer* OBSERVATIONS OF THE HOST GALAXY OF GRB 050904: A METAL-ENRICHED, DUSTY STARBURST AT $z = 6.295$

E. BERGER^{1,2,3}, R. CHARY⁴, L. L. COWIE⁵, P. A. PRICE⁵, B. P. SCHMIDT⁶, D. B. FOX⁷,
S. B. CENKO⁸, S. G. DJORGOVSKI⁹, A. M. SODERBERG⁹, S. R. KULKARNI⁹, P. J. MCCARTHY¹,
M. D. GLADDERS^{1,3}, B. A. PETERSON⁶, AND A. J. BARGER¹⁰

Draft version December 20, 2018

ABSTRACT

We present deep *Hubble Space Telescope* and *Spitzer Space Telescope* observations of the host galaxy of GRB 050904 at $z = 6.295$. The host is detected in the *H*-band and marginally at $3.6 \mu\text{m}$. From these detections, and limits in the z' -band and $4.5 \mu\text{m}$, we infer an extinction-corrected absolute magnitude, $M_{\text{UV}} \approx -20.7$ mag, or $\sim L^*$, a substantial star formation rate of $\sim 15 M_{\odot} \text{ yr}^{-1}$, and a stellar mass of $\text{few} \times 10^9 M_{\odot}$. A comparison to the published sample of spectroscopically-confirmed galaxies at $z > 5.5$ reveals that the host of GRB 050904 would evade detection and/or confirmation in any of the current surveys due to the lack of detectable Ly α emission, which is likely the result of dust extinction ($A_{1200} \sim 1.5$ mag). This suggests that not all luminous starburst galaxies at $z \sim 6$ are currently being accounted for. Most importantly, using the metallicity of $Z \approx 0.05 Z_{\odot}$ inferred from the afterglow absorption spectrum, our observations indicate for the first time that the observed evolution in the mass- and luminosity-metallicity relations from $z = 0$ to $z \sim 2$ continues on to $z > 6$. The ease of measuring redshifts and metallicities from the afterglow emission suggests that in tandem with the next generation ground- and space-based telescopes, a GRB mission with dedicated near-IR follow-up can provide unique information on the evolution of stars and galaxies through the epoch of re-ionization.

Subject headings: gamma rays:bursts — cosmology:observations — galaxies:high-redshift — galaxies:starburst — galaxies:abundances

1. INTRODUCTION

The questions of how and when the universe was re-ionized and the history of galaxy formation and metal enrichment appear to be intimately linked. Observations of $z > 6$ quasars and the cosmic microwave background indicate that re-ionization occurred at $z \sim 7 - 13$ (Becker et al. 2001; Spergel et al. 2006), but most likely not by quasars alone (Fan et al. 2002). Instead, star-forming galaxies and/or massive population III stars may have played a dominant role in this process (e.g., Yan & Windhorst 2004). To assess this possibility it is essential to trace the properties and evolution of galaxies and star formation at $z \gtrsim 6$. In recent years, large surveys using narrow-band Ly α and Lyman drop-out selection have uncovered ~ 100 candidate $z \gtrsim 5.5$ galaxies (e.g., Bouwens et al. 2004b; Dickinson et al. 2004), of which about a half have been confirmed spectroscopically (e.g., Hu et al. 2002; Taniguchi et al. 2005). These surveys provide initial esti-

mates of the star formation rate density and luminosity function at these redshifts (e.g., Bouwens & Illingworth 2006).

Unfortunately, one of the most crucial measurements in the study of galaxy evolution, the metallicity, is beyond the reach of current studies, since at $z \gtrsim 5$ the relevant emission lines¹¹ are very weak and are redshifted to the mid-IR. Moreover, since spectroscopic confirmation relies on Ly α emission, which is easily obscured by dust, the current samples may be intrinsically biased with respect to dust and metallicity. The alternative approach of studying damped Ly α absorbers (DLAs) detected against background quasars also appears to be limited to $z \lesssim 5$ (Prochaska et al. 2003), and is moreover biased in favor of extended halo gas, which at lower redshifts significantly underestimates the disk metallicities. As a result, the apparent evolution in the mass- and luminosity-metallicity relations (M - Z and L - Z) from $z = 0$ to $z \sim 2$ (e.g., Kobulnicky & Kewley 2004; Shapley et al. 2004; Savaglio et al.

¹Observatories of the Carnegie Institution of Washington, 813 Santa Barbara Street, Pasadena, CA 91101

²Princeton University Observatory, Peyton Hall, Ivy Lane, Princeton, NJ 08544

³Hubble Fellow

⁴Spitzer Science Center, California Institute of Technology, Mail Stop 220-6, Pasadena, CA 91125

⁵Institute for Astronomy, University of Hawaii, 2680 Woodlawn Drive, Honolulu, HI 96822

⁶Space Radiation Laboratory, MS 220-47, California Institute of Technology, Pasadena, CA 91125

⁷Division of Physics, Mathematics and Astronomy, 105-24, California Institute of Technology, Pasadena, CA 91125

⁸Department of Astronomy and Astrophysics, Pennsylvania State University, 525 Davey Laboratory, University Park, PA 16802

⁹RSAA, ANU, Mt. Stromlo Observatory, via Cotter Rd, Weston Creek, ACT 2611, Australia

¹⁰Department of Astronomy, University of Wisconsin-Madison, 475 North Charter Street, Madison, WI 53706

¹¹These include [O II] $\lambda 3727$, [O III] $\lambda \lambda 4959, 5007$, [N II] $\lambda 6584$, and the hydrogen Balmer lines.

2005; Erb et al. 2006) cannot be traced to $z > 5$, where such information should shed light on the initial stages of mass build-up and metal enrichment.

For many years it has been speculated that GRBs should exist at $z > 6$ and can therefore provide an alternative way to study re-ionization and to select star-forming galaxies. A truly unique and exciting aspect of GRBs is that spectroscopy of their bright afterglows can easily provide a redshift measurement from UV metal absorption features and/or Ly α absorption, bypassing the reliance on faint Ly α emission lines. More importantly, GRB absorption spectroscopy also provides a measure of the metallicity and kinematics of the interstellar medium *at the location where active star formation is taking place*, and may potentially provide direct information on the nature of the massive progenitor itself. This powerful probe of the metallicity in star forming galaxies, and its redshift evolution, is now being routinely used for a rapidly-growing sample at $z \sim 2-4$ (e.g., Berger et al. 2005; Chen et al. 2005; Starling et al. 2005).

The hope of extending this approach to $z > 6$ was finally realized with the discovery of GRB 050904 at $z = 6.295$, and spectroscopic observations of its afterglow. Here we present *Hubble Space Telescope* and *Spitzer Space Telescope* follow-up observations of the host galaxy of GRB 050904 and discuss its properties in the context of the spectroscopically-confirmed $z > 5.5$ galaxies discovered to date. We find that the host is a $\sim L^*$, low mass, and modestly dusty starburst galaxy with a high specific star formation rate. Combining these results with the absorption-line metallicity, we place the first point on the $M-Z$ and $L-Z$ diagrams of $z > 5$ galaxies, and find that the evolution in these relations continues beyond $z \sim 2$.

2. OBSERVATIONS

GRB 050904 was detected by the *Swift* satellite on 2005, Sep. 4.078 UT (Cusumano et al. 2006). The burst redshift was photometrically estimated to be $z \approx 6.2 - 6.5$ (Price et al. 2005; Tagliaferri et al. 2005; Haislip et al. 2006), and was later confirmed spectroscopically to be $z = 6.295$ (Kawai et al. 2006), making it the highest redshift GRB observed to date. The afterglow absorption spectrum also revealed a damped Ly α absorber with $\log N(\text{HI}) \approx 21.6$, a metallicity of $Z \approx 0.05 Z_{\odot}$, and appreciable dust depletion (Totani et al. 2005; Kawai et al. 2006).

2.1. Hubble Space Telescope

We observed the position of GRB 050904 with HST as part of a program to study the host galaxies of $z > 6$ GRBs (GO 10616). The observations were performed with the Advanced Camera for Surveys (ACS) on 2005, Sep. 26.87 UT, and with the Near Infrared Camera and Multi-Object Spectrometer (NICMOS) on Sep. 27.28 UT. A total of 4216 and 10240 s were obtained in the WFC/F850LP and F160W filters, respectively.

We processed the data using the `multidrizzle` routine (Fruchter & Hook 2002) in the `stsdas` package of IRAF. The ACS images were drizzled using `pixfrac=0.8` and `pixscale=1.0`, resulting in a final pixel scale of $0.05''$

pixel $^{-1}$. The NICMOS images were first re-processed with an improved dark frame created from the HUDF using the IRAF task `calnica` in the `nicmos` package. The resulting images were then drizzled using `pixfrac=0.7` and `pixscale=0.5`, leading to a final pixel scale of $0.1''$ pixel $^{-1}$.

Astrometry was performed relative to a K -band image of the afterglow taken with the Infrared Telescope Facility (Haislip et al. 2006). A total of five objects in common to the IRTF and NICMOS images were used resulting in a 1σ astrometric uncertainty of about $0.05''$. In the NICMOS image we identify a single object coincident with the afterglow position at (J2000) $\alpha=00^{\text{h}}54^{\text{m}}50.846^{\text{s}}$, $\delta=+14^{\circ}05'09.92''$ ($0.08''$ south-east of the afterglow position); see Figure 1. No corresponding object is detected in the ACS image.

Photometry of the object was performed using the zero-points of Sirianni et al. (2005), resulting in $m_{\text{AB}}(\text{F850LP}) > 27.0$ mag (3σ) and $m_{\text{AB}}(\text{F160W}) = 26.1 \pm 0.2$ mag ($0.13 \pm 0.025 \mu\text{Jy}$). An extrapolation of the afterglow flux in the H -band to the time of our observation using the measured decay index of $\alpha = -2.4$ ($F_{\nu} \propto \nu^{\alpha}$; Tagliaferri et al. 2005; Haislip et al. 2006), indicates an expected brightness $m_{\text{AB}}(\text{F160W}) = 26.8 \pm 0.15$ mag, suggesting that about half of the detected flux is due to residual afterglow emission.

We investigated this in more detail by modeling the surface brightness of the object using the GALFIT software (Peng et al. 2002) with a point spread function generated with the Tiny Tim package¹². We use three models: (i) a point-source with $m_{\text{AB}}(\text{F160W}) = 26.8$ mag appropriate for the predicted afterglow brightness, (ii) a point-source with the brightness as a free parameter, and (iii) a point-source with $m_{\text{AB}}(\text{F160W}) = 26.8$ mag and an exponential disk with the brightness and scale length as free parameters. The results of the three fits are shown in Figure 2. We find that models (i) and (ii), for which $m_{\text{AB}}(\text{F160W}) = 26.3 \pm 0.1$ mag, leave significant residuals, indicating the presence of an extended source underlying the GRB position. Model (iii), on the other hand, fully accounts for the observed surface brightness profile, resulting in a host galaxy brightness of $m_{\text{AB}}(\text{F160W}) = 26.7 \pm 0.2$ mag and a scale length of $0.6 \pm 0.3''$. We therefore conclude that the host galaxy contributes about 50% of the flux at the time of our observations.

2.2. Spitzer Space Telescope

As part of the same program (GO 20000) we also observed the field of GRB 050904 with the Infrared Array Camera (IRAC; Fazio et al. 2004) on *Spitzer* in all four channels (3.6, 4.5, 5.8 and $8.0 \mu\text{m}$) on 2005, Dec. 25 UT. The field lies in a region with “medium”-level zodiacal background and cirrus of 34 MJy/sr at $24 \mu\text{m}$ and 9.6 MJy/sr at $100 \mu\text{m}$ on the date of the observations. We used 100 s integrations with 72 medium scale dithers from the random cycling pattern for total on-source integration times of 7200 s at each passband. These nominal 3σ point source sensitivity limits are 0.26, 0.49, 3.3 and $4.2 \mu\text{Jy}$, respectively.

Starting with the S13.2.0 pipeline processed basic cali-

¹²<http://www.stsci.edu/software/tinytim/tinytim.html>

brated data (BCD) sets we corrected the individual frames for muxbleed and column pull down using software developed for the Great Observatories Origins Deep Survey. Due to the presence of bright stars in the field, many of the frames at 3.6 and 4.5 μm also showed evidence for “muxstripping”. This was removed using an additive correction on a column by column basis (J. Surace, priv. comm.). The processed BCD frames were then mosaicked together using the MOPEX routine (Makovoz & Marleau 2005) and drizzled onto a 0.6'' grid. Astrometry was performed relative to the HST/ACS image using 70 common objects, resulting in an rms uncertainty of 0.07'' (3.6 μm) and 0.09'' (4.5 μm).

Photometry at the position of the host galaxy was performed in fixed circular apertures of 1.2'' radius with appropriate beam size corrections applied as stated in the *Spitzer* Observer’s Manual. The presence of brighter sources within $\sim 7''$ of the host position required that we fit for the wings of the point spread function from those sources. We find a marginal detection of the host with $0.17 \pm 0.09 \mu\text{Jy}$ at 3.6 μm , and 3σ upper limits of 0.4 μJy at 4.5 μm , 2.7 μJy at 5.8 μm , and 2.5 μJy at 8.0 μm . With the observed afterglow spectral index, $\beta_\nu = -1.25$ ($F_\nu \propto \nu^{\beta_\nu}$; Tagliaferri et al. 2005; Haislip et al. 2006), we find that the expected 3.6 μm afterglow flux at the time of our observation is negligible, $\lesssim 0.005 \mu\text{Jy}$.

3. HOST GALAXY PROPERTIES

Using the observed fluxes and upper limits (Figure 3) we now investigate the physical properties of the host galaxy¹³. We begin by estimating the host extinction using (i) the difference between the observed and expected¹⁴ afterglow spectral indices, $\beta_\nu = -1.25$ and -0.55 , respectively (Tagliaferri et al. 2005; Haislip et al. 2006), and (ii) the host UV slope (the β_λ - A_{1600} relation; Meurer et al. 1999). The former approach indicates that for a Calzetti (1997) extinction curve $A_V \approx 0.3$ mag, or at the observed F160W and F850LP bandpasses, $A_{2200} \approx 0.7$ mag and $A_{1400} \approx 1.2$ mag. With the latter approach we find $\beta_\lambda \gtrsim -1.5$ and hence $A_{1600} = 4.43 + 1.99\beta_\lambda \gtrsim 1.4$ mag, in rough agreement with the afterglow-based results; here β_λ is defined such that $F_\lambda \propto \lambda^{\beta_\lambda}$. We note that the extinction estimates agree with the significant dust depletion inferred from the afterglow absorption spectrum (Kawai et al. 2006).

At the redshift of the host the observed 3.6 μm band roughly traces the rest-frame optical B -band, leading to an extinction-corrected absolute magnitude, $M_{\text{AB}}(B) \approx -20.7$ mag. The rest-frame UV magnitude, traced by the observed F160W band, is $M_{\text{AB}}(2200) \approx -20.8$ mag, or $M_{\text{AB}}(1400) \gtrsim -20.7$ mag if we use the F850LP limit. These values correspond to a luminosity, $L \approx 1.5L^*$ compared to the luminosity function of $z \sim 6$ candidates in the HUDF (based on photometric redshifts alone; Bouwens & Illingworth 2006), or about $0.7L^*$ when compared to the luminosity function of $z \sim 3 - 4$ Lyman break galaxies

¹³We use the standard cosmological parameters: $H_0 = 70 \text{ km s}^{-1} \text{ Mpc}^{-1}$, $\Omega_m = 0.27$, and $\Omega_\Lambda = 0.73$, which lead to $d_L = 1.95 \times 10^{29} \text{ cm}$ and $1'' = 5.76 \text{ kpc}$ at $z = 6.295$.

¹⁴The value of -0.55 is inferred from the optical time decay rate and the typical assumption of $\nu_m < \nu_{\text{opt}} < \nu_c$, where ν_m and ν_c are the synchrotron peak and cooling frequencies, respectively.

(LBGs; Steidel et al. 1999). Thus, the host of GRB 050904 is roughly an L^* galaxy.

The host star formation rate (SFR) can be estimated from the measured UV luminosity and the conversion relation of Kennicutt (1998). Based on the F160W flux, we find $L_\nu(2200) = (4.6 \pm 1.3) \times 10^{28} \text{ erg s}^{-1} \text{ Hz}^{-1}$, or $\text{SFR} = 6.5 \pm 1.8 M_\odot \text{ yr}^{-1}$. The extinction-corrected rate is about $15 M_\odot \text{ yr}^{-1}$ using the value of A_{2200} inferred above. These values can be contrasted with the limit of $\lesssim 0.8 M_\odot \text{ yr}^{-1}$ inferred from the lack of detectable Ly α emission in the absorption spectrum of GRB 050904 (Totani et al. 2005). The discrepancy can be easily explained in terms of dust absorption of the Ly α photons, providing additional support to the significant extinction inferred from the afterglow spectral slope, the host UV spectral slope, and the depletion pattern.

Incorporating the *Spitzer* data, we provide rough constraints on the stellar mass of the host galaxy. Given the low signal-to-noise we do not attempt real model fits, but instead we adopt a $Z = 0.2 Z_\odot$, Salpeter IMF template from the Bruzual & Charlot (2003) library along with representative values of the mass, stellar population age, and extinction. An IGM absorption model (Madau 1995) has also been incorporated in the SED. The models, shown in Figure 3, indicate that for $A_V \sim 0.3$ mag, as inferred above, the stellar mass ranges from about 10^9 to $4 \times 10^9 M_\odot$ as we vary the stellar population age from 20 to 100 Myr and span the range of uncertainty in the 3.6 μm flux. For a larger extinction, $A_V \sim 1.6$ mag and an age of 5 Myr we find a mass of about $2 \times 10^9 M_\odot$. We therefore conclude that the stellar mass is $\sim \text{few} \times 10^9 M_\odot$, similar for example to the value derived for the $z = 6.56$ galaxy HCM 6A (Chary et al. 2005), while the stellar population age is likely 10 – 100 Myr.

Finally, the inferred scale length for the host galaxy based on the GALFIT model presented in §2 is $r_e = 3.4 \pm 1.7 \text{ kpc}$, consistent with the median value of about 2 kpc for GRB host galaxies at $\langle z \rangle \sim 1.5$ (Wainwright et al. 2005), as well as with the median value of about 1 kpc for i -band drop-outs in the HUDF (Bouwens et al. 2004a).

To summarize, we find that the host galaxy of GRB 050904 is an L^* starburst galaxy with a mass similar to that of the LMC, with interstellar gas enriched to about $0.05 Z_\odot$ (Kawai et al. 2006), and with appreciable dust depletion and extinction.

4. DISCUSSION AND FUTURE DIRECTIONS

GRB 050904 is by far the highest redshift spectroscopically-confirmed burst observed to date, and its host is so far the only $z > 5$ galaxy for which an estimate of the metallicity is available. Given the relatively small number of spectroscopically-confirmed galaxies at $z > 5.5$, it is instructive to compare the properties of a GRB-selected galaxy to those selected through narrow-band Ly α imaging or the Lyman drop-out technique. In Figure 4 we compare some of the basic properties, which

are available for the latter samples, namely the rest-frame absolute magnitudes and UV/Ly α star formation rates. We find that in the published sample, only 14 galaxies are located at higher redshift than the host of GRB 050904. In terms of UV luminosity, the host of GRB 050904 is fainter than about 85% of all the known galaxies, and it has a star formation rate lower than about 70% of all the galaxies.

On the other hand, we stress that the host of GRB 050904 would evade detection or confirmation in the current surveys since its Ly α line flux is very low, $\lesssim 1.7 \times 10^{-18}$ erg cm $^{-2}$ s $^{-1}$ Å $^{-1}$ (Kawai et al. 2006). This is most likely due to absorption by dust as inferred from the afterglow spectral index, the host UV slope, and dust depletion in the absorption spectrum. And yet the host of GRB 050904 is roughly an L^* galaxy with an appreciable star formation rate (as evidenced by the UV luminosity and the occurrence of a GRB) and a substantial gas reservoir as inferred from the neutral hydrogen column density of $\log N(\text{HI}) \approx 21.6$. Naturally, a much larger sample is required to accurately assess the relative contribution of similar galaxies to the star formation budget at $z \sim 6$, but it is clear that with the ability to measure redshifts independent of Ly α emission, GRBs may provide the cleanest handle on obscured star formation at these redshifts.

We now turn to a comparison of the metallicity, mass and luminosity of the host of GRB 050904 to those of lower redshift galaxies in an attempt to provide a first test of evolution in the M - Z and L - Z relations from $z \sim 1 - 2$ to $z > 5$. First, we provide a note of caution that we are comparing a metallicity derived from absorption lines (in this case [S/H] since sulfur is a non-refractory element) to the oxygen abundance derived from emission lines using the R_{23} and $N2$ methods. In the case of quasar DLAs metallicities a nearly 1 dex discrepancy has been noted compared to emission line metallicities. However, unlike quasar sight lines which preferentially probe halo gas, GRB sight lines probe star forming regions, much like emission lines diagnostics. This is supported by observations of systematically higher metallicities as a function of redshift for GRB-DLAs compared to QSO-DLAs (Berger et al. 2005). Thus, the comparison to emission line metallicities is most likely robust, and the only remaining caveat is that the inferred metallicity potentially represents the star forming region local to the GRB, and not the average metallicity of all H II regions in the galaxy. In the absence of additional information, we take the inferred metallicity of $[\text{S}/\text{H}] = -1.3 \pm 0.3$ to be representative.

In Figure 5 we plot the metallicity of the host of GRB 050904 versus luminosity and stellar mass as inferred in §3. For comparison we plot the same data for $z \sim 0.1$ galaxies in the Sloan Digital Sky Survey (Tremonti et al. 2004), $z \sim 0.3 - 1.0$ galaxies from the Gemini Deep Deep Survey, the Canada-France Redshift Survey, and the Team Keck Redshift Survey (Kobulnicky & Kewley 2004; Savaglio et al. 2005), $z \sim 1.0 - 1.5$ galaxies from the DEEP2 survey (Shapley et al. 2005), and $z \sim 2.3$ UV-selected galaxies (Erb et al. 2006). As noted by the aforementioned authors, there is clear evolution in both the M - Z and L - Z relations in the sense that galaxies of a given mass/luminosity have lower metallicities at progres-

sively higher redshifts. The implications of this evolution, and of the M - Z and L - Z relations themselves, are a matter of current investigation, and here we simply note that the host of GRB 050904 indicates that this trend likely continues to much higher redshifts.

Specifically, for galaxies of a similar brightness to the host of GRB 050904 the mean metallicity evolves from $\sim 2 Z_{\odot}$ at $z \sim 0.1$ to $\sim 1 Z_{\odot}$ at $z \sim 0.7$ and $0.4 Z_{\odot}$ at $z \sim 2.3$. A similar trend is observed with mass. The host of GRB 050904, with $Z \sim 0.05 Z_{\odot}$ continues this trend. In fact, the data for GRB 050904 are in good agreement with the empirical time evolution model of the M - Z relation derived by Savaglio et al. (2005), which indicates that for $\log M \sim 9.5$ the expected metallicity at $z = 6.3$ is about $0.1 Z_{\odot}$.

The detection of additional GRBs at $z \sim 6$ will allow us to examine in detail whether the M - Z and L - Z relations actually exist at those redshifts, and if they in fact follow the evolutionary trend observed at lower redshifts. Moreover, with the ability to probe galactic-scale outflows in absorption, we can determine whether the origin of these relations is rooted in higher gas fractions for lower mass galaxies, or outflows from their shallower potential wells — a matter of current debate (McGaugh & de Blok 1997; Tremonti et al. 2004; Erb et al. 2006). This applies to the growing sample of GRB absorption spectra at $z \sim 2 - 4$ as well, which can both fill in the gap from $z \sim 2$ to $z \sim 6$, and through near-IR spectroscopy of the host galaxies allow us to compare emission- and absorption-derived metallicities at $z \sim 2 - 3$, and directly assess the existence of any systematic differences.

We conclude by noting that GRB selection of $z \sim 6$ galaxies is roughly as efficient as other techniques: GRB 050904 required about 6 hr for the afterglow identification and spectroscopy (Tagliaferri et al. 2005; Haislip et al. 2006; Kawai et al. 2006), and 6 HST orbits, compared to an average of ~ 10 hr of large telescope time to locate and confirm a $z \sim 6$ galaxy in other surveys (Bouwens et al. 2004b; Hu et al. 2004; Taniguchi et al. 2005). As demonstrated in this paper, the real power of GRB selection lies in the relative ease of redshift determination and the reduced influence of dust compared to the reliance on faint Ly α emission, and even more importantly the ability to measure metallicities (and at high spectral resolution, kinematics). With this in mind, we suggest that along with the development of future 20 – 30 m ground-based telescopes and *JWST*, a next-generation GRB mission with higher sensitivity and all-sky coverage, coupled with dedicated near-IR imaging and spectroscopy follow-up from the ground, may provide a complementary window into the evolution and metallicity of the first stars and galaxies.

We thank Lisa Kewley and Alice Shapley for helpful comments on the manuscript. EB acknowledges support by NASA through Hubble Fellowship grant HST-01171.01 awarded by STSCI, which is operated by AURA, Inc., for NASA under contract NAS5-26555. Additional support was provided by NASA through grant HST-GO-10616 from STSCI and through a Spitzer award from JPL/Caltech.

References

- Becker, R. H., et al. 2001, *AJ*, 122, 2850
- Berger, E., Penprase, B. E., Cenko, S. B., Kulkarni, S. R., Fox, D. B., Steidel, C. C., & Reddy, N. A. 2005, *ArXiv Astrophysics e-prints*
- Bouwens, R., & Illingworth, G. 2006, *New Astronomy Review*, 50, 152
- Bouwens, R. J., Illingworth, G. D., Blakeslee, J. P., Broadhurst, T. J., & Franx, M. 2004a, *ApJ*, 611, L1
- Bouwens, R. J., et al. 2004b, *ApJ*, 606, L25
- Bruzual, G., & Charlot, S. 2003, *MNRAS*, 344, 1000
- Bunker, A. J., Stanway, E. R., Ellis, R. S., McMahon, R. G., & McCarthy, P. J. 2003, *MNRAS*, 342, L47
- Calzetti, D. 1997, *AJ*, 113, 162
- Chary, R.-R., Stern, D., & Eisenhardt, P. 2005, *ApJ*, 635, L5
- Chen, H.-W., Prochaska, J. X., Bloom, J. S., & Thompson, I. B. 2005, *ApJ*, 634, L25
- Cuby, J.-G., Le Fèvre, O., McCracken, H., Cuillandre, J.-C., Magnier, E., & Meneux, B. 2003, *A&A*, 405, L19
- Cusumano, G., et al. 2006, *Nature*, 440, 164
- Dickinson, M., et al. 2004, *ApJ*, 600, L99
- Erb, D. K., Shapley, A. E., Pettini, M., Steidel, C. C., Reddy, N. A., & Adelberger, K. L. 2006, *ArXiv Astrophysics e-prints*
- Eyles, L. P., Bunker, A. J., Stanway, E. R., Lacy, M., Ellis, R. S., & Doherty, M. 2005, *MNRAS*, 364, 443
- Fan, X., Narayanan, V. K., Strauss, M. A., White, R. L., Becker, R. H., Pentericci, L., & Rix, H.-W. 2002, *AJ*, 123, 1247
- Fazio, G. G., et al. 2004, *ApJS*, 154, 10
- Fruchter, A. S., & Hook, R. N. 2002, *PASP*, 114, 144
- Haislip, J. B., et al. 2006, *Nature*, 440, 181
- Hu, E. M., Cowie, L. L., Capak, P., McMahon, R. G., Hayashino, T., & Komiyama, Y. 2004, *AJ*, 127, 563
- Hu, E. M., Cowie, L. L., McMahon, R. G., Capak, P., Iwamuro, F., Kneib, J.-P., Maihara, T., & Motohara, K. 2002, *ApJ*, 568, L75
- Hu, E. M., McMahon, R. G., & Cowie, L. L. 1999, *ApJ*, 522, L9
- Kawai, N., et al. 2006, *Nature*, 440, 184
- Kennicutt, R. C. 1998, *ARA&A*, 36, 189
- Kobulnicky, H. A., & Kewley, L. J. 2004, *ApJ*, 617, 240
- Kodaira, K., et al. 2003, *PASJ*, 55, L17
- Kurk, J. D., Cimatti, A., di Serego Alighieri, S., Vernet, J., Daddi, E., Ferrara, A., & Ciardi, B. 2004, *A&A*, 422, L13
- Madau, P. 1995, *ApJ*, 441, 18
- Makovoz, D., & Marleau, F. R. 2005, *PASP*, 117, 1113
- McGaugh, S. S., & de Blok, W. J. G. 1997, *ApJ*, 481, 689
- Meurer, G. R., Heckman, T. M., & Calzetti, D. 1999, *ApJ*, 521, 64
- Nagao, T., et al. 2005, *ApJ*, 634, 142
- Nagao, T., Kawabata, K. S., Murayama, T., Ohyama, Y., Taniguchi, Y., Sumiya, R., & Sasaki, S. S. 2004, *AJ*, 128, 109

- Peng, C. Y., Ho, L. C., Impey, C. D., & Rix, H. 2002, *AJ*, 124, 266
- Price, P. A., Cowie, L. L., Minezaki, T., Schmidt, B. P., Songaila, A., & Yoshii, Y. 2005, *ArXiv Astrophysics e-prints*
- Prochaska, J. X., Gawiser, E., Wolfe, A. M., Castro, S., & Djorgovski, S. G. 2003, *ApJ*, 595, L9
- Rhoads, J. E., et al. 2003, *AJ*, 125, 1006
- Rhoads, J. E., et al. 2004, *ApJ*, 611, 59
- Savaglio, S., et al. 2005, *ApJ*, 635, 260
- Shapley, A. E., Coil, A. L., Ma, C.-P., & Bundy, K. 2005, *ApJ*, 635, 1006
- Shapley, A. E., Erb, D. K., Pettini, M., Steidel, C. C., & Adelberger, K. L. 2004, *ApJ*, 612, 108
- Sirianni, M., et al. 2005, *PASP*, 117, 1049
- Spergel, D. N., et al. 2006, *ArXiv Astrophysics e-prints*
- Stanway, E. R., et al. 2004, *ApJ*, 604, L13
- Starling, R. L. C., et al. 2005, *A&A*, 442, L21
- Steidel, C. C., Adelberger, K. L., Giavalisco, M., Dickinson, M., & Pettini, M. 1999, *ApJ*, 519, 1
- Stern, D., Yost, S. A., Eckart, M. E., Harrison, F. A., Helfand, D. J., Djorgovski, S. G., Malhotra, S., & Rhoads, J. E. 2005, *ApJ*, 619, 12
- Stiavelli, M., et al. 2005, *ApJ*, 622, L1
- Tagliaferri, G., et al. 2005, *A&A*, 443, L1
- Taniguchi, Y., et al. 2005, *PASJ*, 57, 165
- Totani, T., Kawai, N., Kosugi, G., Aoki, K., Yamada, T., Iye, M., Ohta, K., & Hattori, T. 2005, *ArXiv Astrophysics e-prints*
- Tremonti, C. A., et al. 2004, *ApJ*, 613, 898
- Wainwright, C., Berger, E., & Penprase, B. E. 2005, *ArXiv Astrophysics e-prints*
- Westra, E., et al. 2005, *A&A*, 430, L21
- Yan, H., & Windhorst, R. A. 2004, *ApJ*, 600, L1

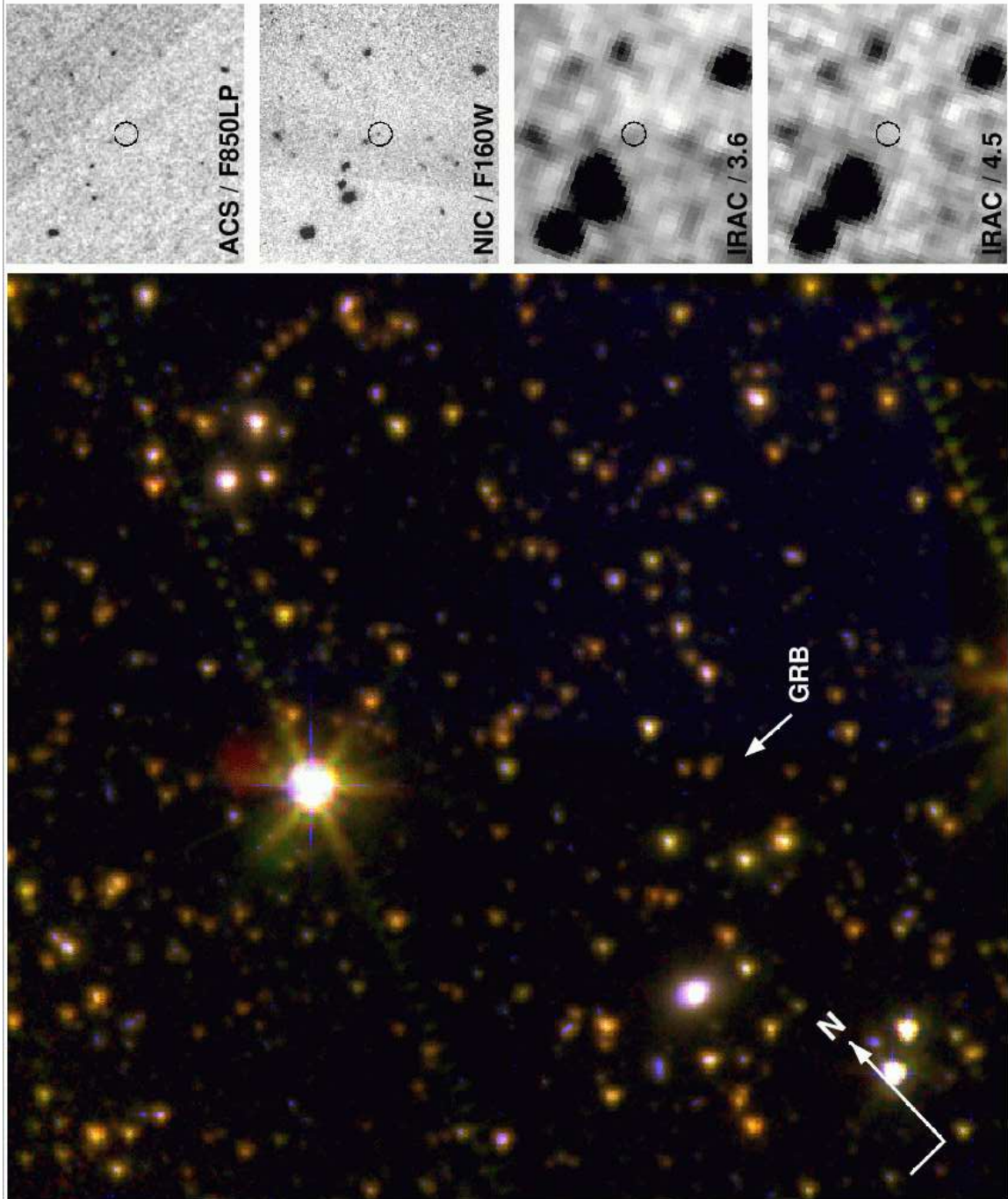


FIG. 1.— A color composite HST+*Spitzer* image of the field of GRB 050904. The panels on the right provide a zoom-in on the position of the host galaxy in each of the four available bandpasses. The host is clearly detected in the NICMOS/F160W image (with an afterglow contamination of about 50%; see §2), and is marginally detected at 3.6 μm .

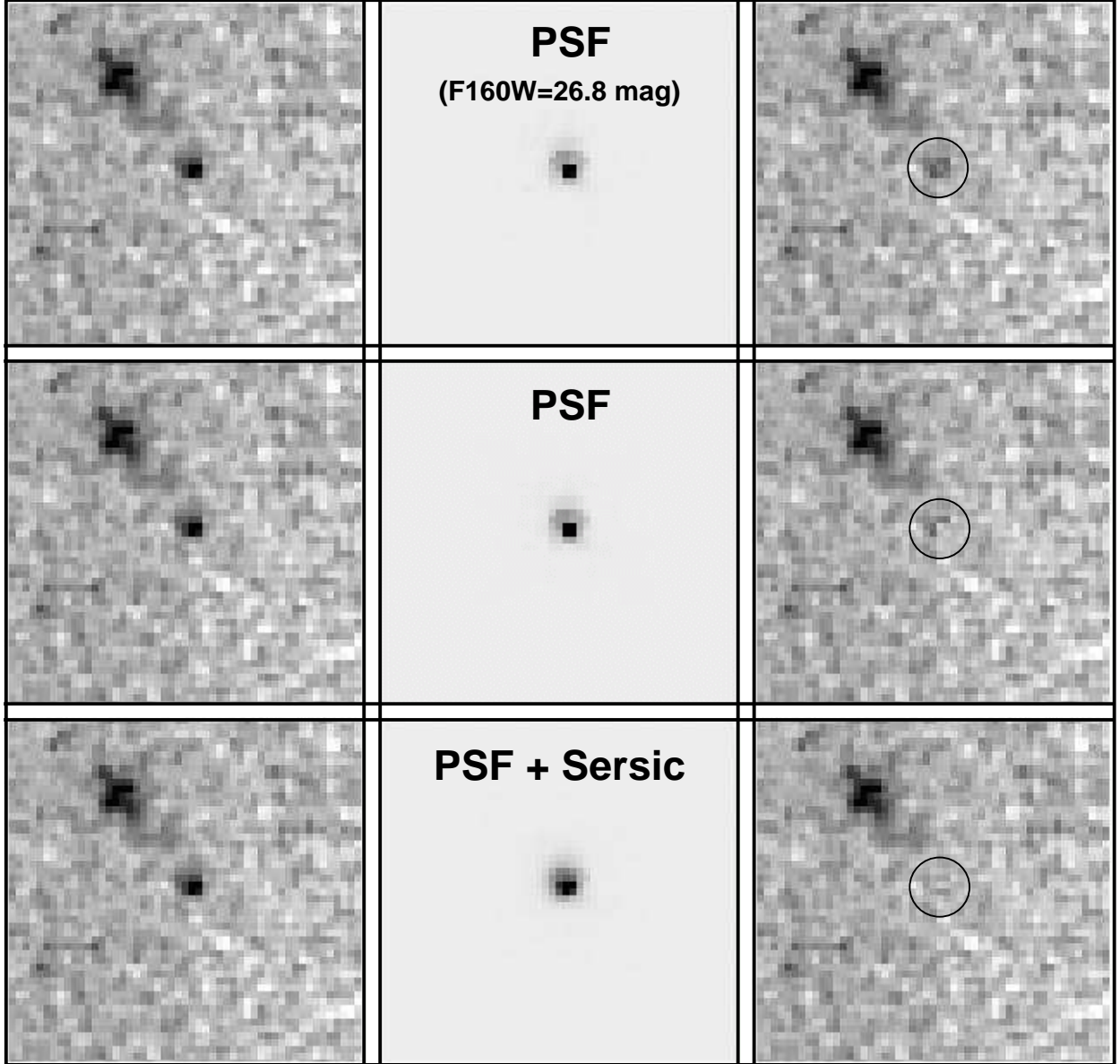


FIG. 2.— Model-fitting of the source coincident with GRB 050904 using three models in GALFIT: (Top) point source with $m_{\text{AB}}(\text{F160W}) = 26.7$ mag as expected from the measured afterglow decay rate; (middle) point source with the brightness as a free parameter; and (bottom) a point source with $m_{\text{AB}}(\text{F160W}) = 26.8$ mag and an exponential disk with the brightness and scale length as free parameters. The middle column shows the resulting model source in each case, while the right column is the residual image. Clearly, a point source alone does not provide an adequate fit, particularly at the expected flux level. Instead an extended source which contributes about half the total flux is required.

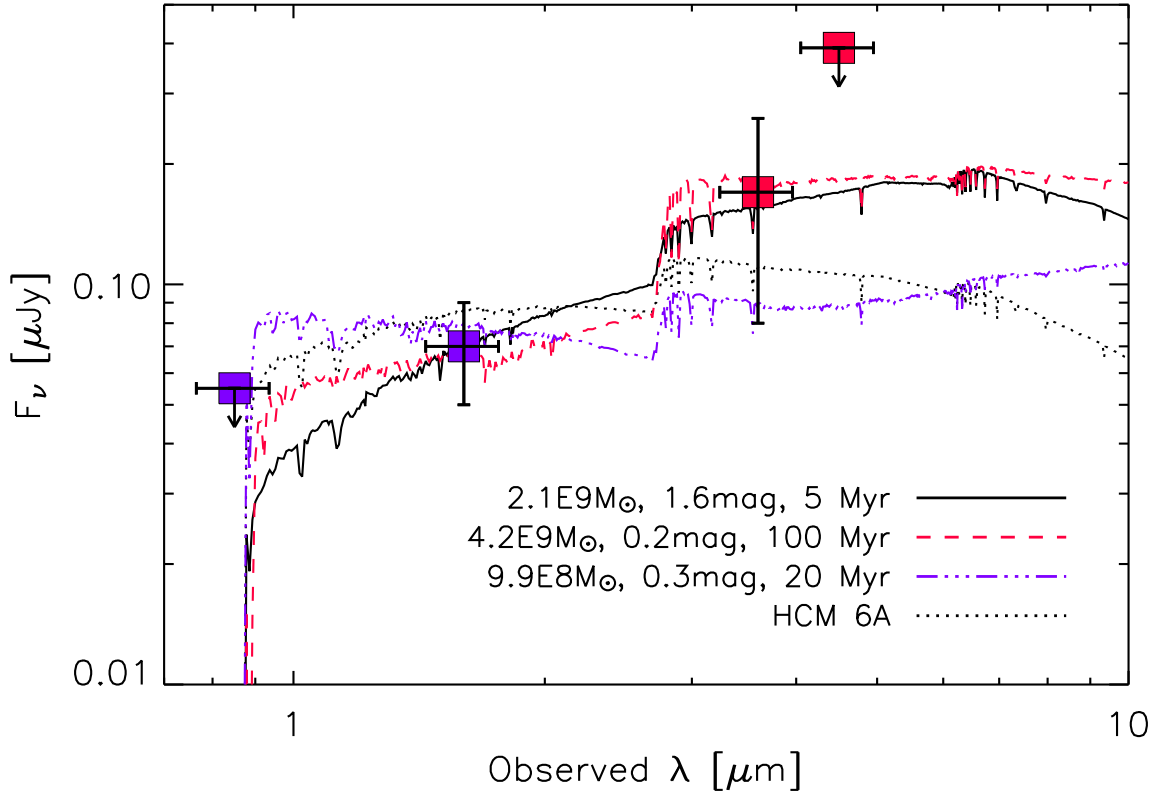


FIG. 3.— Spectral energy distribution of the host galaxy of GRB 050904 from HST (blue) and *Spitzer* (red) data. Three representative SEDs are shown (see §3 for details) with model parameters given in the figure. The models with $A_V \sim 0.2 - 0.3$ mag are based on the extinction inferred from the afterglow emission. For comparison, the dotted line represents the best-fit model to the SED of the $z = 6.56$ galaxy HCM 6A (redshifted to $z = 6.295$) with an age of 5 Myr, $A_V = 1.0$ mag, and $M = 8.4 \times 10^8 M_{\odot}$ (Chary et al. 2005).

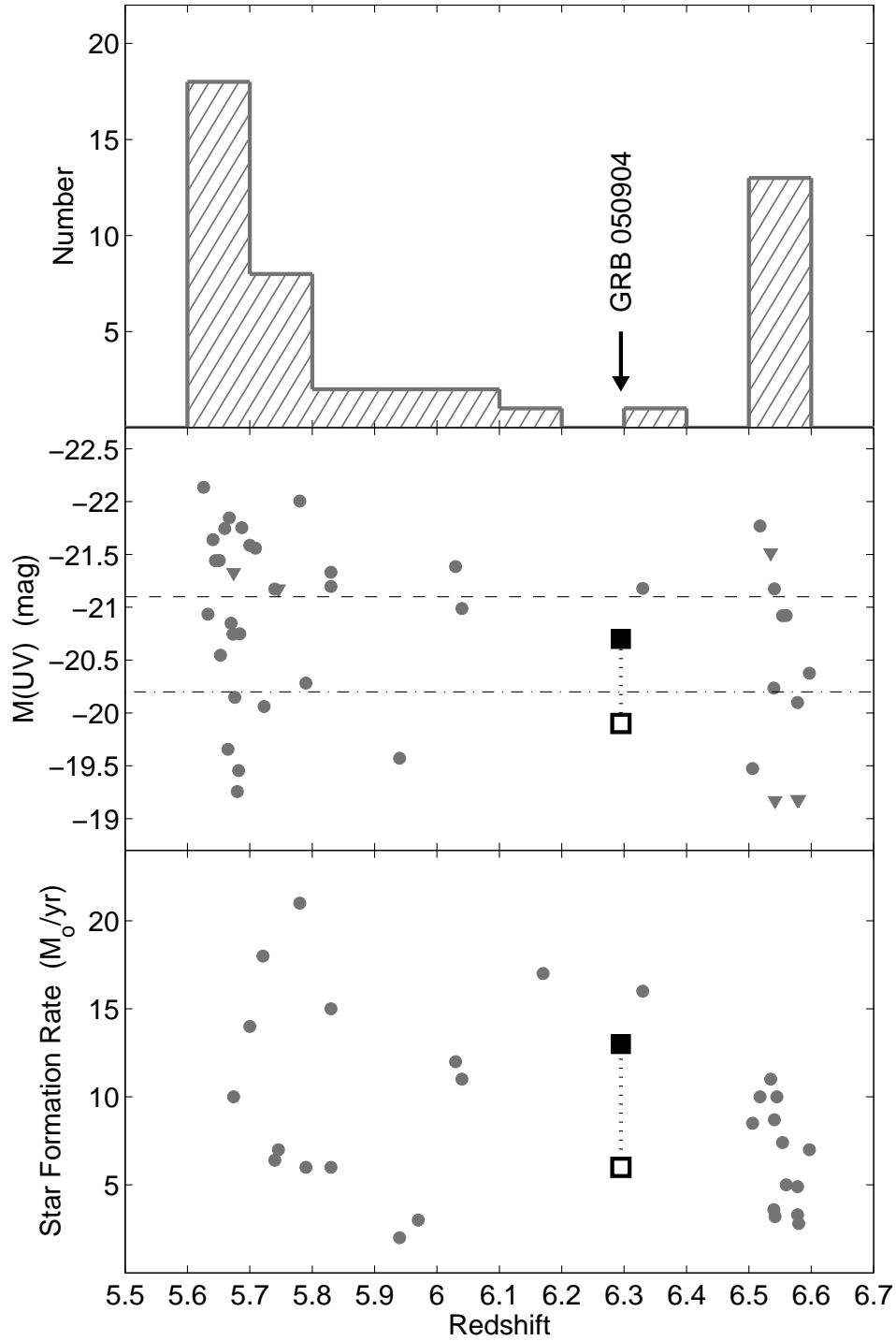


FIG. 4.— The inferred properties of the host of GRB 050904 compared to the published sample of spectroscopically-confirmed galaxies at $z > 5.5$ (Hu et al. 1999, 2002; Bunker et al. 2003; Cuby et al. 2003; Kodaira et al. 2003; Rhoads et al. 2003; Dickinson et al. 2004; Hu et al. 2004; Kurk et al. 2004; Nagao et al. 2004; Rhoads et al. 2004; Stanway et al. 2004; Chary et al. 2005; Eyles et al. 2005; Nagao et al. 2005; Stern et al. 2005; Stiavelli et al. 2005; Taniguchi et al. 2005; Westra et al. 2005). Open and filled black squares designate raw and extinction-corrected quantities, respectively, for the host galaxy. Both detections (circles) and upper limits (triangles) are shown for the distributions of redshifts, absolute rest-frame UV magnitudes, and star formation rates. The dashed line in the middle panel designates an M^* galaxy at $z \sim 3-4$ (Steidel et al. 1999), while the dash-dotted line is M^* for $z \sim 6$ candidates in the HUDF (Bouwens & Illingworth 2006).

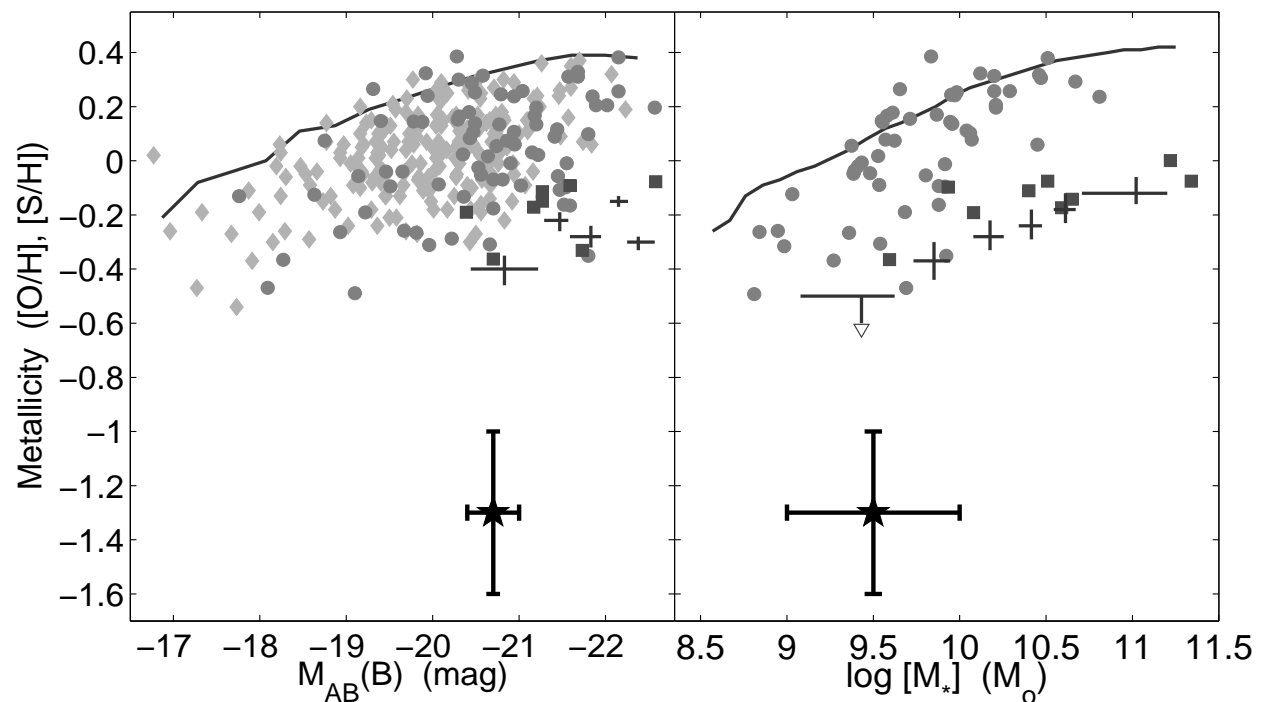


FIG. 5.— Metallicity as a function of luminosity (left) and mass (right) for the host of GRB 050904 using the $[S/H]$ value inferred from the afterglow absorption spectrum (Kawai et al. 2006). Also shown are emission line oxygen abundances for galaxies from GDDS and CFRS at $z \sim 0.4 - 1.0$ (circles; Savaglio et al. 2005), TKRS at $z \sim 0.3 - 1.0$ (diamonds; Kobulnicky & Kewley 2004), the DEEP2 survey at $z \sim 1.0 - 1.5$ (squares; Shapley et al. 2005), and a compilation of 87 LBGs at $z \sim 2.3$ (error bars; Erb et al. 2006). The gray lines represent the relations derived for $z \sim 0.1$ galaxies in the SDSS (Tremonti et al. 2004).